Journal of Molecular Liquids 385 (2023) 122321

Contents lists available at ScienceDirect

Journal of Molecular Liquids

journal homepage: www.elsevier.com/locate/molliq

Modeling of polymer-enzyme conjugates formation: Thermodynamic perturbation theory and computer simulations

Halyna Butovych, Yurij V. Kalyuzhnyi *, Taras Patsahan, Jaroslav Ilnytskyi

Institute for Condensed Matter Physics of the National Academy of Sciences of Ukraine, 1 Svientsitskii St., Lviv, 79011, Ukraine

A B S T R A C T

A simple model for the formation of the polymer-enzyme conjugates has been proposed and described using corresponding modification of the Wertheim's first-order thermodynamic perturbation theory (TPT) for the system of associating chain molecules. A set of computer simulation data for the polymer chains containing various number of functional groups was generated and used to testify the accuracy of the theoretical results. Predictions of the present theoretical approach are more accurate than that of the conventional TPT and are in a very good agreement with the computer simulation data. In particular, the theory is able to account for the difference in the position of the polymer functional groups along its backbone.

1. Introduction

The application of enzymes in chemical industry is of great interest and is constantly developing. This is primarily because of unique catalytic properties of enzymes, which allow them to be considered as an environmentally friendly alternative to many traditional toxic and hazardous chemistry based technologies. One of the areas of such application is converting cellulose biomass into biofuel. The enzymatic biocatalysis is pivotal in the production of first and second generation bioethanol from cellulose using a mixture of different types of enzymes, the so-called cellulases (endocellulases, cellobiohydrolases, beta-glucosidases) [1]. Such kind of enzymes are involved in the process of cellulose hydrolysis, where they synergistically break polysaccharide chains into monosaccharide and oligosaccharide molecules, from which ethanol is subsequently produced by fermentation. Despite the attractiveness of this approach, there is still the problem of efficiency and commercial viability of this technology [2]. A number of strategies exists to increase a catalytic efficiency of enzymes [3]. One of the most promising approaches is immobilization of enzymes on scaffolds [4–8] like polymers [9], nanoparticles [10] and microgels. For instance, it was found that the synthetic enzyme-polymer conjugates mimicking natural cellulosomes can exhibit a sufficiently higher catalytic activity in cellulose hydrolysis when compared to the dispersions of totally free enzymes [5–7,9]. This, obviously, indicates a higher synergy level between enzymes constrained into groups. Moreover, the enzymes captured on scaffolds can be more easily retrieved for the subsequent reuse. It was also observed that enzymes in complexes with brush-like polymers have a higher thermal stability [11,12]. We propose the very basic coarse-grained model to describe a mixture of enzyme globules and multifunctional polymer chains and report theoretical and computer simulation study of the corresponding conjugation process in a system. Brush copolymers are mimicked by the linear flexible chains of spherical beads with the side chains accounted for implicitly. It is assumed that some of the polymer blocks can bear functional groups specific to active sites (patches) located at enzyme molecule, which can bind to the polymer by affinity interactions [5,13]. Enzyme globules are represented by the hard spheres with one active site (patch). Although the model is rather simple and contains relatively small number of the potential model parameters, it is still enough general to capture the key features enabling one to describe the immobilization process of enzymes on polymer scaffolds. It is also conforms to the common understanding of the modeling of the binding processes, which occur between proteins and polymers and discussed in a number of experimental [11,14–17] and theoretical [18,19] studies. Simplicity of the model enable us to develop theoretical approach, which can be successfully used to describe effects due to the difference in the number and distribution of the functional groups along the polymer backbone. We note in passing that currently the theory, which is able to generate sufficiently accurate results for the model at hand, is not available.

In this study we are focused on the development of the model and its theoretical description in the context of the polymer-enzyme conjugation process. Keeping this goal in mind we extend and apply the first order multi-density thermodynamic perturbation theory (TPT) in combination with multi-density integral-equation theory of

* Corresponding author.
E-mail addresses: yukal@icmp.lviv.ua (Y.V. Kalyuzhnyi), tarpa@icmp.lviv.ua (T. Patsahan).

https://doi.org/10.1016/j.molliq.2023.122321
Received 5 February 2023; Received in revised form 15 May 2023; Accepted 9 June 2023
Available online 14 June 2023

Wertheim [20–22] and perform detailed computer simulation study of the model. Our theoretical and computer simulation results are compared and the accuracy of the theoretical predictions is examined. The models similar to the one suggested here have been used earlier to describe effects of aggregation and association in the surfactant systems, alkanols, organic acids, aminoacids, etc (see [23–27] and references therein). In these studies the constituents of the system were modeled by the associating totally flexible chains of spherical Lennard-Jones (LJ) monomers (beads). Association similar to the one in the currently study occurs due to the off-center short-ranged square-well bonding sites (patches) placed on the surface of certain monomers. For the theoretical description the authors have been using TPT with the reference system represented by the fluid of the LJ monomers. The theory, being relatively successful in describing the models with bonding sites placed on the terminal beads of the chains, appears much less accurate if bonding sites were located on the intermediate beads [28–30]. This drawback of the theory is due to the "single bond" approximation utilized in the TPT, i.e. bonding abilities of each of the sites of the monomer do not depend on the bonding state of the rest of the sites [20–22]. There are two possibilities to improve performance of the theory: to apply the higher-order approximations in the framework of the TPT or to use the better choice for the reference system. Unfortunately, the former option is not much feasible, since it requires the application of the higher-order reference system correlation functions, which restrict practical application of this scheme for the second order case [22]. To achieve the higher accuracy using the low-order version of the TPT in many cases it is more efficient to stick with the former option. This route was undertaken in [31–37] to account for the effects of changes in the system excluded volume upon association. In this study we propose to use the reference system represented by the fluid of non-associating chain molecules. Somewhat similar approach was used to correct TPT predictions for the low-density behavior of the equation of state for the chain fluids [38,39]. However, to the best of our knowledge this idea has not been used for the description of the associating chains, in particular when association occurs at the intermediate monomers of the chain. In addition, in the majority of these studies, the properties of the reference fluid were calculated using the fit of the corresponding computer simulation results. Here description of the reference system is carried out analytically, using solution of the multi-density Ornstein-Zernike (OZ) equation supplemented by the associative Percus-Yevick (APY) approximation [40–42]. We refer to this version of the TPT as to the modified TPT (mTPT).

The paper is organized as follows. First, in Section 2 we introduce the general model, which can be tackled by the developed theory and applied, in particular, to the problem stated above. Then, we present the theory itself in Section 3. Technical details of computer simulation performed in this study can be found in Section 4. The obtained results are discussed in Section 5 and concluding remarks are provided in the last Section 6.

2. The model

We start with the two-component mixture of flexible chain molecules consisting of tangentially bonded hard-sphere monomers of different size. Both components are, in general, polymer chains and may contain both ordinary (blue in Fig. 2) and adhesive (red and green in Fig. 2) monomers. Adhesive monomers bear single off-center attractive square-well site (patch) representing a functional group, which is randomly located on the surface. This site-site attractive interaction is valid only between the sites, which belong to the chains of different type. In the limiting case of the latter component represented by only one functional monomer this model reduces to the model of polymer-enzyme mixture. In mimicking this case we would like to stress that both real polymeric scaffolds and enzymes are macromolecules with many conformational degrees of freedom, where binding sites can change their position in relation to other constituents due to the conformational changes (see Fig. 1). This effect is accounted for in this model in an effective way, by representing an average shape of the macromolecular groups by spheres and allowing diffusion of the active site on their surface. The pair potential acting between the monomers is

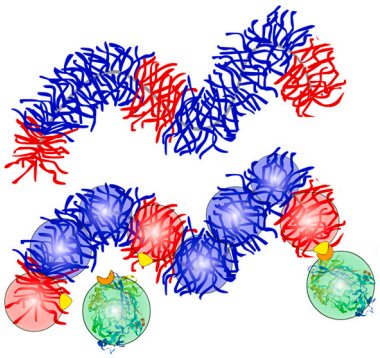

Fig. 1. Sketch of molecular brush block copolymer (top) and its coarse-grained representation with enzyme molecules (bottom).

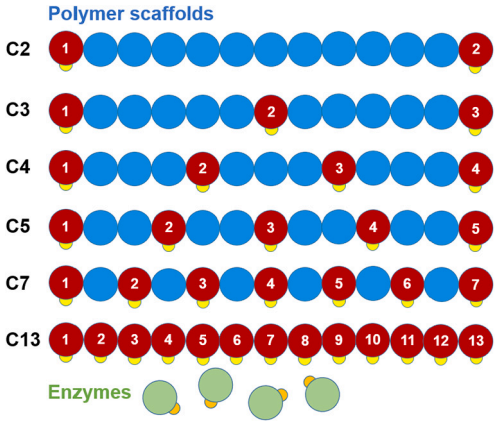

Fig. 2. The models of brush block copolymer scaffolds and enzymes considered in this study. Red circles denote polymer beads bearing the functional group (yellow spot), blue circles – generic polymer beads, green circles – enzyme molecules with the functional group (orange spot).

$$U_{a_i b_j}(12) = U^{(hs)}_{a_i b_j}(r) + U^{(sw)}_{a_i b_j}(12), \tag{1}$$

where $a(b)$ denote the type of the chain and $i(j)$ denote the type of the monomer belonging to the chain of the type $a(b)$,

$$U^{(hs)}_{a_i b_j}(r) = \begin{cases} \infty, & \text{for } r \le \sigma_{a_i b_j} \\ 0, & \text{otherwise} \end{cases}, \tag{2}$$

$$U^{(sw)}_{a_i b_j}(12) \equiv U^{(sw)}_{a_i b_j}(z) = \begin{cases} -(1-\delta_{ab})\epsilon_{a_i b_j}, & \text{for } z \le \kappa \\ 0, & \text{otherwise} \end{cases}, \tag{3}$$

z is the distance between the square-well sites, $\sigma_{a_i b_j}$ is the hard-sphere diameter, $\epsilon_{a_i b_j}$ and κ are the square-well depth and width, respectively. The indices a and b each take the values 1 and 2, and the indices i and j take the values $1, \dots, n_a$ and $1, \dots, n_b$, respectively. Here $n_a(n_b)$ is the number of the monomers in the chain of the type $a(b)$. The system number density is $\rho = \rho_1 + \rho_2$, where ρ_1 and ρ_2 are the number density of the chains of the type 1 and 2, respectively.

3. Theory

Following Wertheim [20,21] we assume that Helholtz free energy A of the mixture at hand can be written as a sum of Helmholtz free energy of the reference system A_{ref} and corresponding contribution due to bonding ΔA_{bond}, i.e.

$$A = A_{ref} + \Delta A_{bond}, \tag{4}$$

where the reference system is represented by the original two-component mixture of hard-sphere chain molecules with $\epsilon_{a_i b_j} = 0$ and for ΔA_{bond} we have

$$\beta \frac{\Delta A_{bond}}{V} = \sum_{a=1}^{2} \rho_a \left[\sum_{i=1}^{n_a} \left(\ln X_{a_i} - \frac{1}{2} X_{a_i} \right) + \frac{1}{2} n_a \right]. \tag{5}$$

Here n_a is the number of the square-well sites located on the chain molecule of the type a and X_{a_i} is the fraction of the molecules of the type a with nonbonded square-well site on the monomer of the type i. These fractions satisfy the mass action law type of the relation

$$X_{a_i} \sum_{b=1}^{2} \rho_b \sum_{j=1}^{n_b} X_{b_j} K_{a_i b_j} + X_{a_i} - 1 = 0, \tag{6}$$

where $K_{a_i b_j}$ characterizes the association between the sites i and j of the chains of the type a and b. According to Wertheim's TPT $K_{a_i b_j}$ is represented by the integral of the product of Mayer function $f_{a_i b_j}^{(sw)}(12) = \exp(-\beta U_{a_i b_j}^{(sw)}(12)) - 1$ and corresponding pair distribution function over configurational space of the two particles. We assume the following approximation for $K_{a_i b_j}$:

$$K_{a_i b_j} = 4\pi \int_{\sigma_{a_i b_j}}^{\sigma_{a_i b_j}+\kappa} r^2 \bar{f}_{a_i b_j}^{(sw)}(r) g_{a_i b_j}^{(ref)}(r) dr, \tag{7}$$

where $g_{a_i b_j}^{(ref)}(r)$ is the monomer-monomer pair distribution function, $\bar{f}_{a_i b_j}^{(sw)}(r)$ is the orientationally averaged monomer-monomer Mayer function

$$\bar{f}_{a_i b_j}^{(sw)}(r) = \frac{(1-\delta_{ab}) F_{a_i b_j}^{(sw)}}{6\sigma_{a_i b_j}^2 r} \left(\kappa + \sigma_{a_i b_j} - r \right)^2 \left(2\kappa - \sigma_{a_i b_j} + r \right) \tag{8}$$

and $F_{a_i b_j}^{(sw)} = e^{\beta \epsilon_{a_i b_j}} - 1$. Our approximation is based on the observation that due to the short-range character of the square-well potential $U_{a_i b_j}(12)$ the only configurations, which give nonzero contribution to the integral $K_{a_i b_j}$ are those when two sites (i, a) and (j, b) are located at a distance of $r \le \kappa$. For this distance the Mayer function takes the constant value, i.e. $f_{a_i b_j}^{(sw)}(12) = F_{a_i b_j}^{(sw)}$ and $K_{a_i b_j}$ can be approximated using expression (7). This approximation is verified by the comparison between theoretical predictions and computer simulations.

3.1. Description of the reference system

Thermodynamic properties of the reference system can be calculated using first-order thermodynamic perturbation theory (TPT) of Wertheim [21,22]. For the Helmholtz free energy of the reference system we have

$$\beta \frac{A_{ref}}{V} = \beta \frac{A_{hs}}{V} - \sum_{a=1}^{2} \rho_a \sum_{i=1}^{n_a - 1} \ln y_{a_i a_{i+1}}^{(hs)}(\sigma_{a_i a_{i+1}}), \tag{9}$$

where $y_{a_i b_j}^{(hs)}(r)$ is the hard-sphere cavity correlation function. The fractions X_{a_i} can be obtained from the solution of equation (6) provided that the value of the integral $K_{a_i b_j}$ (7) is known. To simplify calculation of this integral we assume that the Mayer function $\bar{f}_{a_i b_j}^{(sw)}(r)$ can be approximated by the Dirac delta-function, i.e.

$$\bar{f}_{a_i b_j}^{(sw)}(r) = T_{a_i b_j} \delta(r - \sigma_{a_i b_j}), \tag{10}$$

where

$$T_{a_i b_j} = \sigma_{a_i b_j}^{-2} \int_{\sigma_{a_i b_j}}^{\sigma_{a_i b_j}+\kappa} r^2 \bar{f}_{a_i b_j}^{(sw)}(r) dr. \tag{11}$$

Now for $K_{a_i b_j}$ we have

$$K_{a_i b_j} = 4\pi \sigma_{a_i b_j}^2 T_{a_i b_j} g_{a_i b_j}^{(ref)}(\sigma_{a_i b_j}), \tag{12}$$

where the contact values of the radial distribution functions (RDF) $g_{a_i b_j}^{(ref)}(\sigma_{a_i b_j})$ can be calculated using analytical solution of the polymer Percus-Yevick ideal chain approximation for heteronuclear hard-sphere chain fluids [40–42]

$$\begin{aligned}
\sigma_{a_i b_j} g_{a_i b_j}^{(ref)}(\sigma_{a_i b_j}) &= \frac{\sigma_{a_i b_j}}{1-\eta} + \frac{1}{4} \frac{\rho s_n \sigma_{a_i} \sigma_{b_j}}{(1-\eta)^2} \\
&+ \frac{1}{4(\eta-1)} \sigma_{b_i} \left[\left(1 - \delta_{j1}\right) \frac{\sigma_{b_{j-1}}}{\sigma_{b_j b_{j-1}}} + \left(1 - \delta_{j n_b}\right) \frac{\sigma_{b_{j+1}}}{\sigma_{b_j b_{j+1}}} \right] \\
&+ \frac{1}{4(\eta-1)} \sigma_{a_i} \left[\left(1 - \delta_{i1}\right) \frac{\sigma_{a_{i-1}}}{\sigma_{a_i a_{i-1}}} + \left(1 - \delta_{i n_a}\right) \frac{\sigma_{a_{i+1}}}{\sigma_{a_i a_{i+1}}} \right] \\
&+ \frac{\delta_{ab}}{8\pi\rho_a} \left[\frac{(1-\delta_{1i})(1-\delta_{2i})}{\sigma_{a_i a_{i-1}} \sigma_{a_{i-1} a_{i-2}}} \delta_{ij+2} + \frac{(1-\delta_{i n_a})(1-\delta_{i n_a - 1})}{\sigma_{a_i a_{i+1}} \sigma_{a_{i+1} a_{i+2}}} \delta_{ij-2} \right].
\end{aligned} \tag{13}$$

Here $\eta = \pi/6 \sum_a \rho_a \sum_i \sigma_{a_i}^3$ and $s_n = \pi/\rho \sum_a \rho_a \sum_i \sigma_{a_i}^2$.

4. Computer simulation details

Computer simulation of the model of polymer-enzyme mixture (see Fig. 2) was performed by the method of molecular dynamics (MD) at constant volume and temperature using LAMMPS software package (version 30Nov2020) [44]. To control the temperature during the simulations the Langevin thermostat [43] is applied by introducing friction F_f and stochastic F_r force terms:

$$F_f = -m/\gamma v, \qquad F_r \propto \sqrt{\frac{k_B T m}{\tau_d \delta t}}, \tag{14}$$

which are mutually related through the fluctuation-dissipation theorem and depend on the damping time τ_d (relaxation time).

Since force fields in the MD simulations require continuous pair potentials, the square-well and hard-sphere potentials needed in our theoretical model are substituted by their continuous analogs. For the square-well interaction (3) acting between functional sites of the polymer and enzyme, the original LAMMPS code was extended by implementing the force field [45], which introduces the continuous square well (CSW) pair potential:

$$u_{\mathrm{csw}}(r) = -\frac{1}{2} \epsilon_{\mathrm{csw}} \left[1 - \tanh\left(\frac{(r - r_{\mathrm{w}})}{\alpha} \right) \right]. \tag{15}$$

In contrast to [45], we use more steep square well shape of u_{csw} by choosing $\alpha = 0.001\sigma$. The radius of attractive well was chosen $r_{\mathrm{w}} = 0.12\sigma$, the cutoff radius was 0.17σ, and the attractive well depth ϵ_{csw} was defined as the energy unit. With these parameters the shape of $u_{\mathrm{csw}}(r)$ closely reproduces the conventional square-well potential (3). The positions of all functional sites are restricted to the external surfaces of their host beads by constraining their separation from the respective host center using the SHAKE algorithm with the tolerance 0.0001. Sizes of all beads in the polymer and size of enzyme molecules were taken equivalent and set to σ, which was used as the unit of distances in our simulations. The hard-sphere pair interaction between particles (2) was substituted with the pseudo-hard sphere pair potential (PHS) using the repulsive part of the cut and shifted (50,49)-Mie potential as it was suggested in [46,45]:

$$u_{\mathrm{phs}}(r) = \begin{cases} 50 \left(\frac{50}{49}\right)^{49} \epsilon_{\mathrm{phs}} \left[\left(\frac{\sigma}{r}\right)^{50} - \left(\frac{\sigma}{r}\right)^{49} \right], & r < \frac{50}{49}\sigma \\ 0, & r \ge \frac{50}{49}\sigma \end{cases} \tag{16}$$

Since we considered two different temperatures in our study, i.e. $T^* = 0.12$ and $T^* = 0.09$, parameter ϵ_{phs} of PHS potential was rescaled respectively as $\epsilon_{\mathrm{phs}} = \epsilon_{\mathrm{csw}} T^*/1.5$, where $T^* = k_B T/\epsilon_{\mathrm{csw}}$ was the temperature in

Table 1
Number density of polymer chains taken in each of the models, ρ_p.

C2	C3	C4	C5	C7	C13
0.016	0.015	0.014	0.013	0.012	0.009

reduced units. The intramolecular interactions within polymer chains were modeled by the harmonic bonds $u_{\text{bond}}(r) = K(r - r_0)^2$ with the spring constant $K = 160.0\epsilon_{\text{csw}}/\sigma^2$ and the equilibrium distance $r_0 = \sigma$. The non-bonding interactions u_{csw} and u_{phs} were not take into account between the nearest adjacent beads belonging to the same polymer chain.

The timestep for the velocity Verlet integration of the equations of motion in our simulations was chosen as $\delta t = 0.0001\tau$ and the Langevin damping parameter was set to $\tau_d = 0.1\tau$, where $\tau = (m\sigma^2\epsilon_{\text{csw}}^{-1})^{1/2}$ was the time unit. The small timestep guaranteed a stable binding process between polymer and enzyme molecules, which was noticed in our preliminary runs to be vulnerable at larger timesteps due to the steep pair potentials and very short r_w used in the model.

All simulations of polymer chains and enzyme molecules were performed in the cubic box of the same size $L = 50.0\sigma$ with the periodic boundary conditions applied. A number of particles varied depending on the number densities of polymer and enzyme molecules taken in our study (see Table 1). The maximum number of enzymes (about 15000) was considered in Model C13. The maximum number of polymer chains (2000) was chosen in Model C2, and the minimum of them was in Model C13 (1154). For each set of parameters the simulations were done in three stages. First stage was used to thoroughly mix enzymes with polymers to lose a trace of the initial system, and it was achieved during a short period of 10^6 simulation steps without patches activated. At the second stage the patches were activated and the system was equilibrated during the period required to reach a saturation of bonds creation, which was typically $200 \cdot 10^6$ steps. The third stage contained production runs and it lasted $300 \cdot 10^6$ simulation steps. During the production runs all necessary data were collected at every 10000 steps and averaged.

5. Results and discussion

To illustrate application of the TPT developed above and to systematically access its accuracy we consider the model represented by the two-component mixture of the polymer chain molecules and enzyme monomers i.e. $a = 1$ and $a = 2$, respectively (see Fig. 2). The chains representing polymer scaffolds consist of 13 hard-sphere beads of the size σ with a certain number of the beads bearing functional groups. These beads are distributed along the chain backbone uniformly and symmetrically. Enzyme molecules are represented by the hard spheres of the same size σ and one functional site per each sphere, which can conjugate to the polymer functional group due to the square-well attractive potential. We have studied the models with 2, 3, 4, 5, 7 and 13 polymer beads bearing functional sites and denote them as C2, C3, C4, C5, C7 and C13, respectively (see Fig. 2). The width and depth of the square-well site-site interaction was chosen to be $\kappa = 0.119\sigma$ and $\epsilon_{a_i b_j} = \epsilon$ and we consider two temperatures: $T^* = T/\epsilon = 0.09$ and $T^* = 0.12$.

In Fig. 3 (top panel) we show our results for the average number of bonds per number of polymer functional groups $\xi_p = 1 - X_{2_1}$ for all six types of model at the constant packing fraction of the system $\eta = \pi/6(\rho_e + 13\rho_p)\sigma^3 = 0.126$ and at the fixed ratio $\rho_e/\rho_p = k_p$, where k_p is the number of beads of the chain with functional groups, $\rho_p = \rho_1$ and $\rho_e = \rho_2$. With this choice of the densities the number of enzyme molecules are equal to the total number of polymer beads with the functional groups in the system. At higher temperature ($T^* = 0.12$) one can observe a slight increase of the fraction of bonded enzymes with increasing the number of functional beads per chain. At lower temperature ($T^* = 0.09$) this increase is more pronounced, however only up to

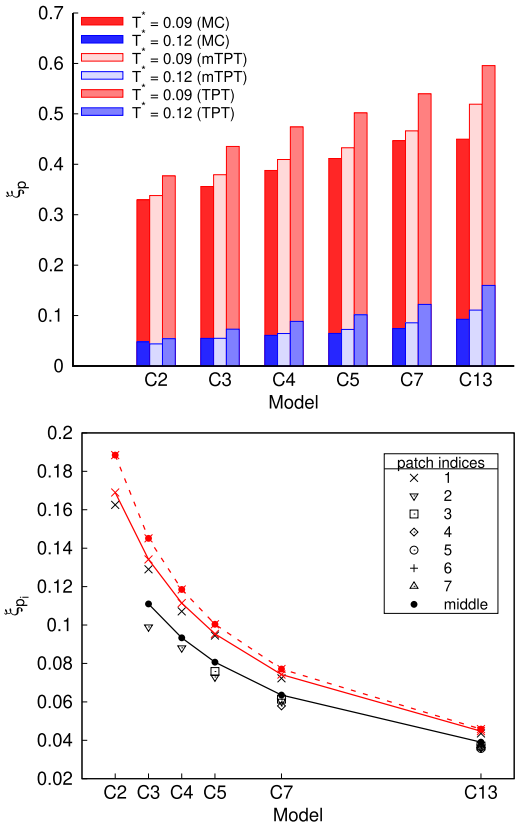

Fig. 3. Top panel: Average number of bonds per number of enzyme molecules for models C2, C3, C4, C5, C7 and C13 at $T^* = 0.09$ (red boxes), $T^* = 0.12$ (blue boxes) and at the fixed packing fraction $\eta = 0.126$ when the total number of polymer functional groups in the system are equal to the number of enzymes, i.e. $n_e = n_p k_p$ (k_p – number of patches per polymer chain, n_e and n_p – number of enzyme and polymer molecules, respectively). Bottom panel: Average number of bonds formed with the selected polymer functional groups per number of enzyme molecules (for $n_e = n_p k_p$), where each functional group index corresponds to its serial number at polymer molecule ($T^* = 0.09$). (see Fig. 2). Here filled red circles and red crosses, connected by the red dashed line, represent results of the TPT, red crosses connected by the red solid line and black filled circles connected by the solid black line represent results of the mTPT. All the rest of the symbols represent computer simulation results.

7 functional beads (Model C7). With further increase of the number of functional beads (Model C13) the fraction of bonded enzyme particles, calculated using LD simulation, remains unchanged. On the other hand, theoretical calculations show further increase of ξ_p. Thus, while at the higher T^* the probability of bonding does not depend much on the number of functional beads on the polymer chain, at the lower temperature it is seen that at large k_p the enzyme molecules begin to partially block each other upon bonding to nearby beads.

In general, predictions of the mTPT are in a good agreement with computer simulation results, except that theoretical predictions for the model C13, where mTPT overestimate the value of ξ_p. This is to be expected, since neither mTPT nor TPT is able to account for the blocking effects mentioned above. Results of the conventional TPT are substantially less accurate. In the same figure (Fig. 3, bottom panel) we present the average number of bonds connected to the particular functional bead on the polymer chain per number of such beads, i.e. $\xi_{p_i} = (1 - X_{1_i})$, $i = 1, \ldots, 13$. One can observe a substantial difference in the fraction of enzymes bonded at the terminal (crosses) and middle (circles) beads of the polymer chain. The difference between fractions of enzymes bonded to the different beads inside the chain is minor. Again, mTPT results are accurate here and in particular the theory is able to reproduce the difference in bonding abilities of the terminal and middle beads of the chain. Due to the choice of the reference sys-

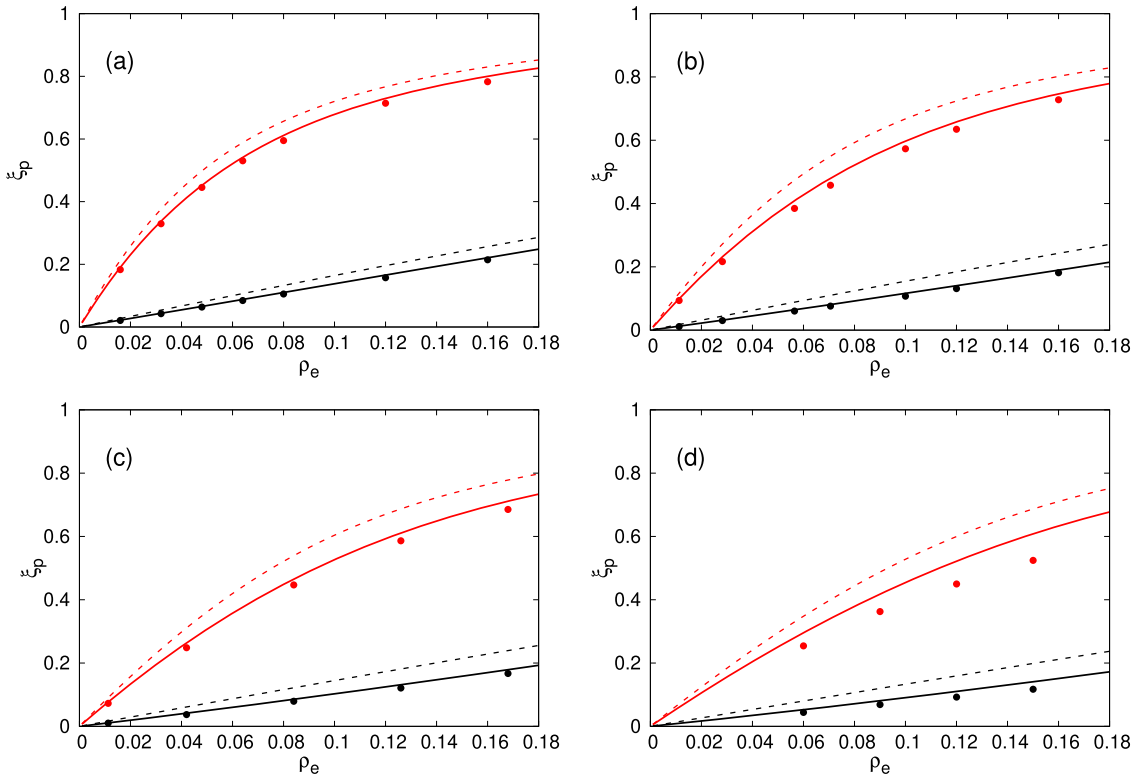

Fig. 4. Number of bonds per number of polymer functional groups X_p vs number density of enzyme molecules ρ_e. On the panels (a), (b), (c) and (d) we show results for the models C2, C4, C7 and C13, respectively. Here solid and dashed lines represent results of the mTPT and TPT, respectively and symbols stand for computer simulation results. Calculations were carried out at $T^* = 0.09$ (red lines and symbols) and $T^* = 0.12$ (black lines and symbols).

tem, represented by the hard-sphere fluid, TPT gives equal values for the fraction of bonded beads regardless of their position in the chain (red crosses and red filled circles in Fig. 3 coincide) and corresponding predictions are much less accurate in comparison with mTPT predictions. According to the ideal chain approximation, used to calculate the structure properties of the reference system, the contact values of the RDF between the enzymes and the middle beads of the polymer chain are equal [47]. As a result, fraction of bonded non-terminal beads predicted by mTPT is the same regardless of their position in the chain. This assumption of the theory is consistent with the undertaken computer simulation results.

Next we have studied the system at fixed densities of the chain molecules ρ_p and different densities of the enzymes ρ_e in the range of $0-0.18$ and two values of the temperature, $T^* = 0.09$ and 0.12. The density of the polymer chains were chosen to be different for each model: (see Table 1). Our theoretical (mTPT) and computer simulation (symbols) results are shown in Fig. 4. In addition, we include results of the conventional TPT approach (TPT), which is based on the application of the hard-sphere reference system. One can observe a very good agreement of our mTPT predictions with the data of computer simulations. On the contrary, the theoretical results of the unmodified version of the TPT are much less accurate.

Finally it is worth noting that the major goal of our study is to present and verify theoretical description of the course grained version of the model for the polymer-enzyme conjugates formation. Parameters of the model have not being suited to any specific enzyme and/or polymer, we are using here certain generic values. However, in a subsequent papers we are planning to apply the theory developed to study formation and properties of the conjugates formed by specific polymer and enzyme molecules. Potential model parameters will be obtained either coarse-graining atomistic force-fields or adjusting theoretical results to corresponding experimental data.

6. Conclusions

We propose a theoretical description for the formation of polymer-enzyme conjugates using a simple model of two-component mixture consisting of flexible hard-sphere chains of polymer bearing a number of uniformly arranged functional groups and hard-sphere enzyme molecules with a single specific site able to conjugate to these groups. Depending on the grafting density of functional groups on the polymers and the polymer-enzymes composition, different number of enzymes can bind to the polymer scaffolds at different places. The model proposed is very simple and include relatively small number of the potential model parameters. The values of these parameters can be adjusted and the model can be used to describe specific enzymes and polymers. Theoretical description of the model was carried out using a corresponding modification of the Wertheim's first-order thermodynamic perturbation theory. To assess the accuracy of the theory we have generated a set of computer simulation data. Our analyses are focused on the abilities of the theory to correctly reproduce the number of the bonds created between enzyme molecules and polymer functional groups differently located along the chain. We have shown that predictions of the present theory are in a very good agreement with corresponding computer simulation and appears to be much more accurate than that of the conventional TPT approach. An important advantage of the developed theory is its simplicity and ability to provide a completely analytical description for the general case of any number of the functional groups at polymer beads and enzymes molecules as well as for different size ratios of them.

CRediT authorship contribution statement

All authors have contributed equally.

Declaration of competing interest

The authors declare that they have no known competing financial interests or personal relationships that could have appeared to influence the work reported in this paper.

Data availability

Data will be made available on request.

Acknowledgements

Yu.K., T.P. and Ja.I. acknowledge CRDF Global Award no. 66705. HB acknowledges financial support from the National Research Foundation of Ukraine (project No. 2020.02/0317).

References

[1] B. Yang, Z. Dai, S.Y. Ding, C.E. Wyman, Biofuels 2 (4) (2011) 421–449.
[2] G. Liu, J. Zhang, J. Bao, Bioprocess Biosyst. Eng. 39 (2016) 133–140.
[3] V. Mbaneme-Smith, M.S. Chinn, Energy Emiss. Control Technol. 3 (2015) 23–44.
[4] N.A. Carter, X. Geng, T.Z. Grove, Protein-Based Engineered Nanostructures, Springer, Cham, 2016, pp. 179–214.
[5] J.E. Hyeon, S.K. Shin, S.O. Han, Biotechnol. J. 11 (11) (2016) 1386–1396.
[6] S. Moraïs, A. Heyman, Y. Barak, J. Caspi, D.B. Wilson, R. Lamed, O. Shoseyov, E.A. Bayer, J. Biotechnol. 147 (3–4) (2010) 205–211.
[7] J. Stern, S. Moraïs, R. Lamed, E.A. Bayer, mBio 7 (2) (2016) e00083-16.
[8] X. Lyu, R. Gonzalez, A. Horton, T. Li, Catalysts 11 (10) (2021) 1211.
[9] O. Zholobko, A. Hammed, A. Zakharchenko, N. Borodinov, I. Luzinov, B. Urbanowicz, T. Patsahan, J. Ilnytskyi, S. Minko, S.W. Pryor, A. Voronov, ACS Appl. Polym. Mater. 3 (4) (2021) 1840–1853.
[10] K. Khoshnevisan, F. Vakhshiteh, M. Barkhi, H. Baharifar, E. Poor-Akbar, N. Zari, H. Stamatis, A.K. Bordbar, Mol. Catal. 442 (2017) 66–73.
[11] N.S. Yadavalli, N. Borodinov, C.K. Choudhury, T. Quiñones-Ruiz, A.M. Laradji, S. Tu, I.K. Lednev, O. Kuksenok, I. Luzinov, S. Minko, ACS Catal. 7 (12) (2017) 8675–8684.
[12] X. Wang, N.S. Yadavalli, A.M. Laradji, S. Minko, Macromolecules 51 (14) (2018) 5039–5047.
[13] A. Rodriguez-Abetxuko, D. Sánchez-deAlcázar, P. Muñumer, A. Beloqui, Front. Bioeng. Biotechnol. 8 (2020) 830.
[14] A. Grotzky, T. Nauser, H. Erdogan, A.D. Schlüter, P. Walde, J. Am. Chem. Soc. 134 (28) (2012) 11392–11395.
[15] G.A. Ellis, W.P. Klein, G. Lasarte-Aragones, M. Thakur, S.A. Walper, I.L. Medintz, ACS Catal. 9 (12) (2019) 10812–10869.
[16] S. Gad, S. Ayakar, Biotechnol. Rep. 32 (2021) e00670.
[17] F. Asaduzzaman, S. Salmon, Mol. Syst. Des. Eng. 7 (11) (2022) 1385–1414.
[18] S. Kondrat, U. Krauss, E. von Lieres, Curr. Res. Chem. Biol. 2 (2022) 100031.
[19] I. Coluzza, P.D. van Oostrum, B. Capone, E. Reimhult, C. Dellago, Phys. Rev. Lett. 110 (7) (2013) 075501.
[20] M.S. Wertheim, J. Stat. Phys. 35 (1984) 19;
M.S. Wertheim, J. Stat. Phys. 35 (1984) 35.
[21] M.S. Wertheim, J. Stat. Phys. 42 (1986) 459;
M.S. Wertheim, J. Stat. Phys. 42 (1986) 477.
[22] M.S. Wertheim, J. Chem. Phys. 87 (1987) 7323.
[23] E.A. Müller, K.E. Gubbins, Ind. Eng. Chem. Res. 40 (2001) 2193.
[24] I.G. Economou, Ind. Eng. Chem. Res. 41 (2002) 953.
[25] P. Paricaud, A. Galindo, G. Jackson, Fluid Phase Equilib. 194 (2002) 87.
[26] S.P. Tan, H. Adidharma, M. Radosz, Ind. Eng. Chem. Res. 47 (2008) 8063.
[27] C. McCabe, A. Galindo, Appl. Thermodyn. Fluids (2010) 215.
[28] E.A. Muller, L.F. Vega, K.E. Gubbins, Mol. Phys. 83 (1994) 1209.
[29] E.A. Muller, L.F. Vega, K.E. Gubbins, Int. J. Thermophys. 16 (1995) 705.
[30] C. Herdes, J.C. Pamies, R.M. Marcos, L.F. Vega, J. Chem. Phys. 120 (2004) 9822.
[31] Y.V. Kalyuzhnyi, G. Stell, M.L. Llano-Restrepo, W.G. Chapman, M.F. Holovko, J. Chem. Phys. 101 (1994) 7939.
[32] T. Urbic, V. Vlachy, Y.V. Kalyuzhnyi, K.A. Dill, J. Chem. Phys. 127 (2007) 174511.
[33] Y.V. Kalyuzhnyi, S.P. Hlushak, P.T. Cummings, J. Chem. Phys. 137 (2012) 244910.
[34] Y.V. Kalyuzhnyi, M. Holovko, T. Patsahan, P.T. Cummings, J. Phys. Chem. Lett. 5 (2015) 4260.
[35] J. Rescic, Y.V. Kalyuzhnyi, P.T. Cummings, J. Phys. Condens. Matter 28 (2016) 41401.
[36] Y. Kalyuzhnyi, A. Jamnik, J. Mol. Liq. 228 (2017) 133.
[37] Y.V. Kalyuzhnyi, A. Jamnik, P.T. Cummings, Soft Matter 13 (2017) 1156.
[38] D. Ghonasgi, W.G. Chapman, J. Chem. Phys. 100 (1994) 6633.
[39] J. Chang, S.I. Sandler, Chem. Eng. Sci. 49 (1994) 2777–9822.
[40] Y.V. Kalyuzhnyi, P.T. Cummings, J. Chem. Phys. 103 (1995) 3265.
[41] Y.V. Kalyuzhnyi, C.T. Lin, G. Stell, J. Chem. Phys. 106 (1997) 1940.
[42] C.T. Lin, Y.V. Kalyuzhnyi, G. Stell, J. Chem. Phys. 108 (1998) 6513.
[43] M.P. Allen, D.J. Tildesley, Computer Simulation of Liquids, Oxford University Press, 2017.
[44] S. Plimpton, Fast parallel algorithms for short-range molecular dynamics, J. Comput. Phys. 117 (1995) 1–19.
[45] J.R. Espinosa, A. Garaizar, C. Vega, D. Frenkel, R. Collepardo-Guevara, J. Chem. Phys. 150 (22) (2019) 224510.
[46] J. Jover, A.J. Haslam, A. Galindo, G. Jackson, E.A. Müller, J. Chem. Phys. 137 (14) (2012) 144505.
[47] Y.V. Kalyuzhnyi, C.T. Lin, G. Stell, J. Chem. Phys. 108 (1998) 6525.